

## Segmentation, tracking and lineage analysis of yeast cells in bright field microscopy images

R. LA BROCCA<sup>(1)</sup>, F. MENOLASCINA<sup>(2)</sup>, D. DI BERNARDO<sup>(1)(2)</sup> and C. SANSONE<sup>(1)</sup>

<sup>(1)</sup> *Dipartimento di Informatica e Sistemistica, Università di Napoli "Federico II"*  
*Via Claudio 21, I-80125, Naples, Italy*

<sup>(2)</sup> *Systems and Synthetic Biology Laboratory, Telethon Institute of Genetics and Medicine*  
*Via Pietro Castellino 111, I-80131, Naples, Italy*

ricevuto il 30 Settembre 2011; approvato l' 1 Dicembre 2011

**Summary.** — Time lapse microscopy images are an important support in quantitative biology. Gene circuit dynamics can be precisely estimated at a single-cell level but automatic cell segmentation and tracking are required due to the large number of cells under study and the large amount of images to be analyzed. Here we present a solution for segmentation, tracking and lineage analysis of yeast cells in bright field, phase contrast microscopy images. The solution is designed to be applied with little effort by biologists thanks to the robust global linking segmentation approach and a pattern recognition-based false-positive detection system. Performance evaluation methods are also introduced and used for a reliable evaluation of our method. Moreover, we show here that our method achieves competitive performances with existing methods without time-consuming optimal parameters search.

PACS 87.18.Vf – Systems biology.

PACS 87.17.Aa – Modeling, computer simulation of cell processes.

### 1. – Introduction

Time lapse microscopy images are used by biologists to study gene circuit dynamics in single cells [1]. Several applications in quantitative biology (*e.g.* systems biology) require cells to be engineered to express fluorescent protein reporters allowing to follow the dynamics of a gene of interest. Microscopy images can be used to obtain quantitative measures of the protein concentration levels over time in each cell through image processing routines. Bright field images are used to track cell movements over time and construct lineage trees reporting mother-daughter relationships between cells while fluorescent field images are used to evaluate the expression level dynamics in every tracked cell. Although humans are good at cell identification, tracking and division detection in image sequences, manual analysis is a tedious, time-consuming and error-prone task. Automatic cell segmentation and tracking, nevertheless, are complex tasks whose success

usually depends on strong assumptions. Many solutions had been developed in this field: watershed and active contours methods represents the state-of-the-art segmentation techniques [2] but they need consistent efforts to adapt to the specific characteristics of the experiment of interest. Existing software, such as *CellTracer* [3] and *CellProfiler* [4], have been found to be heavily dependent on parameters' choice and to possibly perform poorly on new data unless a long search for the optimal parameters set is carried out. This is mainly due to the fact that each experimental context is characterized by its own peculiarities thus making the quest for the parameters-set-fitting-all-situations a task destined to fail. For this reason we focused on a particular bright field image acquisition technique, namely phase contrast. In this context, we developed a solution meant to be robust to experimental variability and able to automatically find the best set of parameters via a pattern recognition approach. Here we argue that the implemented solution can be used by biologist with little knowledge in the field of image processing and allows us to achieve competitive results when compared with best case scenarios of alternative solutions. The paper is organized as follows: in sect. 2 we present the solution developed for segmentation, tracking and lineage analysis of yeast cells in phase contrast microscopy images. In sect. 3 the methods for a reliable performance evaluation are presented, while in sect. 4 the results of the performance evaluation on a reference dataset are reported together with a comparative evaluation of our method versus *CellTracer*. Finally, sect. 5 draws some conclusions.

## 2. – Methodological approach

Cell tracking and lineage reconstruction in microscopy image sequences can be performed in two steps:

1. the first step consists in the segmentation of each frame in order to extract the position of the cells;
2. the second step consists in detecting single-cell movements through the identification of same cells present in two consecutive frames.

The solution presented in this paper had been developed with real-time applications in mind. More specifically, we aimed at making the solution robust to image sequence variability in terms of intensity contrast between the pixels belonging to the cells and the pixels belonging to the background. This is a key factor in the field of biology: experimental conditions may vary dramatically on the basis of the optical configurations (magnification used, lens numerical aperture) and of supporting materials (coverslip chamberslide *vs.* microfluidic devices). In order to make our solution as insensitive as possible to these factors, we based our segmentation method on global edge linking and on a machine learning-based false-positive detection system. In this discussion we will focus on yeast cell tracking and cell division detection. The solution requires the user to input very few parameters specification and a binary classifier training. The training set construction can be done using a graphical user interface that hides the technical aspects in feature extraction.

**2.1. Segmentation.** – Yeast cells in bright field phase contrast images occur in clustered, low-intensity, convex and often quasi-circular shapes surrounded by a white halo (see fig. 1a). The contrast between the pixels belonging to the cells and the pixels belonging to the halos is usually so high that edge points can be detected by the evaluation of the

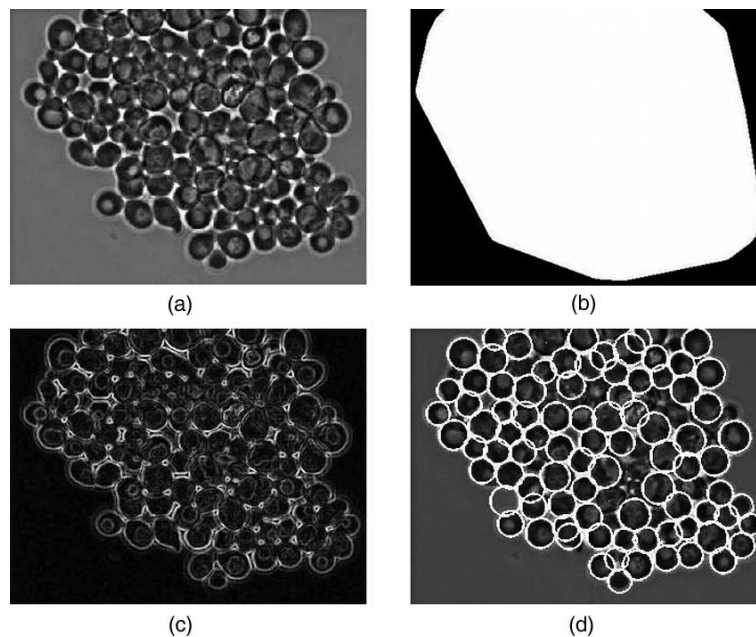


Fig. 1. – Yeast cells in a bright field phase contrast microscopy image (a), the mask that select the region where cells are present (b), the gradient magnitude image (c), circles detected by CHT superimposed on the original image (d).

magnitude of the gradient calculated in each point of the image (see fig. 1b). Due to the particular cell shape, edge points can be connected with the Circular Hough Transform (CHT) [5]. CHT can detect almost all the cells in the images, even when cells edges overlap (see fig. 1c); unfortunately the CHT algorithm is computationally expensive (both in memory and time) and shows poor specificity capabilities. Therefore, in order to limit the time required for a full computation to complete we designed a preprocessing of the image that first selects the regions in the image where cells are located. Those regions are selected with a mask, obtained as a result of a thresholding operation, performed by using the Otsu method [6, 7], and of the union of the convex hull of the connected component in order to remove holes [7]. False detections are reduced as a result of the segmentation of these regions only. Moreover, since the area of the regions in the image containing cells is smaller than the area of the background, the computational time of the CHT is considerably reduced. The segmentation process gives at each frame  $t$  a set of detected objects  $o^t$ . Those objects represent regions likely to feature at least a cell. As CHT is used to detect cells, those regions are circular shaped and their positions are the coordinates in the plane of the centers of the circles.

**2.2. False-positives detection system.** – In agreement with common practices in image processing, we define as false positives the detections that do not map to a unique cell. False-positives reduction is necessary since wrong cells may confuse the tracking algorithm. In order to deal with this task we designed and developed a false-positive detection system based on Decision Trees; this tool asks the user to provide a set of bright field images sampled from in-house time-lapse experiments and to perform an interactive segmentation validation process, so that a training set can be constructed. Thanks to

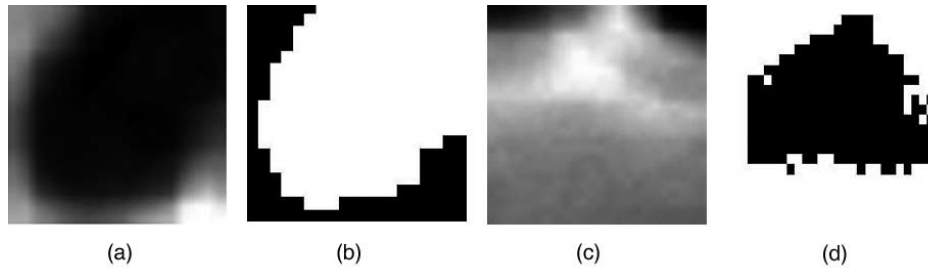


Fig. 2. – In case of correct detection (a) the extracted mask contains a blob in the center that selects the pixels belonging to the detected cell (b). In case of a false positive (c), the extracted mask contains no centered blobs (d).

this approach, the trained classifier is tailored on the particular characteristics of the in-house experiments (optical configurations, supporting materials, etc.). The system is composed by three modules:

- User segmentation validation (USV) module
- Feature extraction (FE) module
- Classifier training (CT) module

USV presents to the user the set of bright field images specified for training with unfiltered segmentation results superimposed. The user selects the correct detections and the unselected ones are considered as false positives. As a result of the user validation process a set of labeled objects is obtained. Each label can assume a Boolean value indicating whether the corresponding object is a correct detection or a false positive. FE module builds the training set from the labeled objects. For each labeled object FE module performs thresholding and morphological operations in order to obtain the subregion whose pixels belongs to cells (see fig. 2) and extract the following features:

- the average intensity value of the extracted subregion
- the proportion of the pixels in the convex hull containing the subregion that are also in the subregion (solidity)
- the displacement from the centroid specified by the object to the center of the subregion, divided by the radius specified by the object
- the proportion of the pixels in the region that are also in the subregion
- the histogram (with 10 bins) of the intensity of the region represented by the object.

The CT module trains a classifier with the training set created by the FE module. A Decision Tree (DT) [8] is chosen because a biologist expert can interpret the rules in the tree coming from the training process.

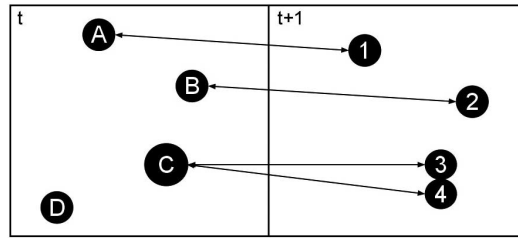


Fig. 3. – Objects detected in two consecutive frames. The arrows identify the correspondences spotting the minimum cost configuration.

**2.3. Tracking and lineage.** – Since yeast cells make small frame-to-frame movements, tracking and cell division detection can be performed by finding the correspondences between the objects detected in two consecutive frames spotting a minimum cost configuration (see fig. 3). This association cost increases as long as the displacement between the centroids of the corresponding objects. The minimum cost configuration can be determined by setting up and solving a linear programming problem (LPP). Given a frame  $t$ , the next one  $t + 1$ , the sets

$o^t \equiv \{o_1^t, \dots, o_n^t\}$  objects detected in frame  $t$ ,

$o^{t+1} \equiv \{o_1^{t+1}, \dots, o_m^{t+1}\}$  objects detected in frame  $t + 1$ ,

$p^t \equiv \{p_1^t, \dots, p_n^t\}$  positions of the objects detected in frame  $t$ ,

$p^{t+1} \equiv \{p_1^{t+1}, \dots, p_m^{t+1}\}$  positions of the objects detected in frame  $t + 1$ ,

and the correspondence matrix  $C^{n \times m}$  having the elements

$c_{i,j} = 1$  if  $o_i^t$  corresponds to  $o_j^{t+1}$ ,

$c_{i,j} = 0$ , otherwise,

$i = 1, \dots, n; j = 1, \dots, m$ ,

the LPP to solve is

$$\min \sum_{j=1}^n \sum_{k=1}^m \phi_{j,k} c_{j,k},$$

s.p.

$$\sum_{j=1}^n c_{j,k} = 1; k = 1, \dots, m,$$

$$c_{j,k} \geq 0; j = 1, \dots, n; k = 1, \dots, m$$

with  $\phi_{j,k} = \|p_j^t - p_k^{t+1}\|$ .

The equality constraints impose that each object detected in frame  $t + 1$  has to correspond to one and only one object detected in frame  $t$ . Each object detected in frame, indeed, can correspond to one, many or no object detected in frame  $t + 1$ . A set of tracked objects  $o_{tracked}$  is initialized in the first frame and updated in the following ones. The correspondence matrix, coming from the solution of the LPP, reports the correspondences between the object tracked up to the frame preceding the current one and the object

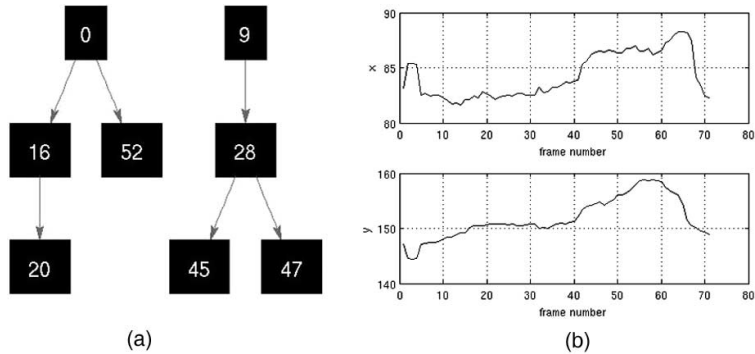


Fig. 4. – Lineage trees (a) from the tracking/lineage process and the trajectories of a tracked cell (b).

detected in the current frame. For each object  $o_{tracked,j}$  corresponding to only one object detected in the current frame,  $p_{tracked,j} = p_k^t$  is set. If  $o_{tracked,j}$  corresponds to more than one element in  $o^t$ , its position is set to the position of the corresponding element at minimum distance. The other corresponding objects represent new cells, and are assumed to be daughters of the cell represented by  $o_{tracked,j}$ . If  $o_{tracked,j}$  corresponds to no object in  $o^t$ , the value of an associated counter is decremented. That counter is initialized for all tracked object with the maximum allowed segmentation misses value. If a counter reaches the value zero, the associated tracked object is removed from  $o_{tracked}$ . The result of the tracking/lineage process is a set of lineage trees (see fig. 4a). Each node in the trees represents a cell and each edge a mother-daughter relation between the cells represented by the connected nodes. By using the software we developed, the user can visualize the trajectory performed by the corresponding cell by clicking on a node (see fig. 4b).

### 3. – Performance evaluation

The quality of a method for the segmentation, tracking and lineage analysis can be evaluated just looking at the visual output generated by its implementation, but a reliable performance evaluation requires hand segmentation/tracking/lineage data (reference data). A set of performance indexes and a method for their evaluation given the reference data and the output data is also required. Reference data are provided by a human expert and are stored as a set  $s^t$  composed by sets of objects for all frames of the reference image sequence; a set of the trajectories of the centroids of each hand-detected and tracked cell; lineage trees reporting mother-daughter relations. Given the set  $o^t$  containing objects detected in frame  $t$  by the segmentation algorithm,  $o_i^t \in o^t$  is a correct detection of the cell represented by  $s_j^t \in s^t$  if  $\|p(s_j^t) - p(o_i^t)\| < \epsilon$  where  $\epsilon$  is the maximum allowed displacement from the reference object centroid and the detected object centroid. Objects in  $s^t$  with no correspondence with any element in  $o^t$  are false negative. Objects in  $o^t$  with no correspondence with any element in  $s^t$  are false positive. The correspondences between elements in  $s^t$  and  $o^t$  are determined with the same approach used in the tracking/lineage method. Once the correspondences for all the frames of the reference image sequence have been determined, the performance of the segmentation algorithm is evaluated by setting the total number of correspondences  $c$ , the total number of reference objects  $m$  and the total number of detected objects  $n$ , and by calculating precision, recall

and  $F$ -measure ( $F$ ) values [9] as

$$\text{precision} = \frac{c}{m}; \quad \text{recall} = \frac{c}{n}; \quad F\text{-measure} = \frac{2 * \text{precision} * \text{recall}}{\text{precision} + \text{recall}}.$$

The segmentation accuracy for each object in  $o^t$  that finds a correspondence with a reference object is calculated as

$$\text{acc}_{i,j} = \frac{A(r(o_i^t) \cap r(s_j^t))}{A(r(o_i^t) \cup r(s_j^t))}$$

with  $s_j^t, o_i^t$  corresponding objects in frame  $t$ , and  $r(s_j^t), r(o_i^t)$  the masks that select in frame  $t$  the regions represented by  $s_j^t$  and  $o_i^t$ .  $A(r)$  is the area of the region selected by  $r$ . Tracking performance evaluation is analogous to segmentation performance evaluation. The correspondences between the reference trajectories and the ones provided by the tracking algorithm are determined solving the same LLP discussed above but with the costs calculated as

$$\phi_{j,k} = \|\bar{s}_j - \bar{t}_i\| + \frac{|\text{len}(s_j) - \text{len}(t_i)|}{\text{ov}(s_j, t_i)} * 100$$

with,  $\bar{s}_j, \bar{t}_i$  the overlapping parts of the reference trajectory  $s_j$  and the provided one  $t_i$ ;  $\text{len}(s_j), \text{len}(t_i)$  lengths of  $s_j$  and  $t_i$ ;  $\text{ov}(s_j, t_i)$  numbers of frame in which the trajectories overlap. Precision, recall and  $F$ -measure values are calculated as well as the performance indexes shown below for each corresponding pair:

- Start frame displacement (SFD)
- End frame displacement (EFD)
- minimum, maximum, average and standard deviation of the  $x$  components of the difference of the overlapping parts of the corresponding trajectories
- minimum, maximum, average and standard deviation of the  $y$  components of the difference of the overlapping parts of the corresponding trajectories

The solution of the LPP used in tracking performance evaluation can be seen as a set of correspondences that selects the matching subsets from the reference data and algorithm provided object sets. This information is used for the lineage construction performance evaluation for the evaluation of precision, recall and  $F$ -measure in terms of correct mother-daughter relationships. SFDs can be used to track the delays in new cells detections.

#### 4. – Experimental results

The training set for the false positives detection system was built on a selection of image sequences available from our experiments. It consists of 6866 elements, 2955 of which are true positives. The confusion matrix of the trained classifier is shown in the table I.

The misclassification rate evaluated with a leave-one-out cross validation was 0.1. The method has been then tested with reference to data coming from two image sets,

TABLE I. – *Confusion matrix of the trained classifier, evaluated on the training set.*

	True positives	False positives
True positives	2879	76
False positives	100	3811

parts of two independent experiments. The first image set is a 50 frames sequence from one of our experiments. The second one is a 50 frames sequence extracted from the sample set available in *CellTracer* website [10] and is used for a comparative evaluation of the performance of *CellTracer* and our method against the same reference data. Both this sets refer to the part in the corresponding experiments characterized by a high cell replication. As can be seen in tables II and III, the method discussed in this paper achieves good performances in segmentation and tracking of yeast cells. Our method detects cell divisions as well, but the performances in mother-daughter relationships detection are not so good. CHT combined with false positive detection works well in detecting the presence and the location of cells but more can be foreseen in segmentation accuracy improvement.

One of the strengths of our method is that few parameters have to be specified. CTH is robust against image contrast and noise to signal ratio variability. That is the why our solution works well on a large variety of bright field phase contrast microscopy experiments. On the other hand, region based segmentation methods need more effort in finding the correct parameters to make them working on the particular experiment. This is an important drawback in real-time tracking applications. Table IV shows the comparative results of the performance evaluation process of *CellTracer*'s and our method against the sample image sequence available in *CellTracer* website [10]. The false positives detection system was not used here because *CellTracer*'s sample images present different cell size and contrast characteristics with respect to the samples we used to train our classifier in the previous experiments. On the other hand, there was not a set of *CellTracer*'s images different from the data used for comparing the two methods, that could be employed for training our DT classifier without biasing the comparison. Thus, a simple thresholding on the average intensity of the region represented by the objects provided from segmentation algorithm has been used. Although the use of the false positives

TABLE II. – *Segmentation method performance indexes. Performance indexes evaluated with no false-positive elimination are reported in brackets.*

Precision	Recall	$F$	Min acc.	Max acc.	Avg. acc.
0.92 (0.53)	0.88 (0.92)	0.90 (0.67)	0.18 (0.12)	0.95 (0.94)	0.74 (0.73)

TABLE III. – *Tracking method performance indexes. Performance indexes evaluated with no false-positive elimination are reported in brackets.*

Tracking			Lineage		
Precision	recall	$F$	Precision	recall	$F$
0.87 (0.42)	0.80 (0.95)	0.83 (0.58)	0.21 (0.27)	0.43 (0.3)	0.28 (0.33)

TABLE IV. – A comparison of the performance indexes evaluated for *CellTracer* and our solution.

	Segmentation			Tracking		
	Precision	Recall	$F$	Precision	Recall	$F$
<i>CellTracer</i>	0.98	0.82	0.89	0.80	0.80	0.80
This	0.89	0.92	0.90	0.83	0.95	0.89

detection system would increase the performance of our method in terms of precision, the overall performance of our method and *CellTracer*'s method are comparable in terms of segmentation, while our method performs definitely better than *CellTracer* in terms of tracking results.

## 5. – Conclusions and future work

In this paper a robust method for yeast cell segmentation, tracking and lineage analysis is presented. A reliable performance evaluation method is also introduced. The results of the comparative analysis we carried out confirms the competitive performance of our approach, making it a good choice for biologists looking for simple and out-of-the-box solutions. These results encourage further improvements in segmentation accuracy and mother-daughter relationships detections.

## REFERENCES

- [1] LOCKE J. C. W. and ELOWITZ M. B., *Nat. Microbiol.*, **7** (2009) 383.
- [2] SRINIVASA G., FICKUS M. and KOVACEVIC J., *Active contour-based multiresolution transforms for the segmentation of fluorescence microscope images*, in *Proc. SPIE*, **6701** (2007) 18.
- [3] WANG Q. *et al.*, *Cytometry Part A*, **77** (2010) 101.
- [4] CARPENTER A. E. *et al.*, *Genome Biol.*, **7** (2006) R100.
- [5] PEDERSEN S. J. K., *Circular hough transform Aalborg University, Vision, Graphics, and Interactive Systems*, **R100** (1991).
- [6] OTSU N., *Automatica*, **11** (1975) 285.
- [7] GONZALEZ R. C. and WOODS R. E., *Digital Image Processing*, 3rd edition (Prentice Hall) 2008.
- [8] STEINBERG D. and COLLA P., *CART classification and regression trees, San Diego, CA: Salford Systems*, **7** (1997).
- [9] MAKHOUL J. *et al.*, *Performance measures for information extraction Broadcast News Workshop 99 Proceedings*, **7** (1999) 249.
- [10] <http://www.stat.duke.edu/research/software/west/celltracer/download/yeast.zip>.